Structure and Properties of a Semifluorinated Diblock Copolymer Modified Epoxy Blend

Connie Ocando,[†] Elena Serrano,[†] Agnieszka Tercjak,[†] Cristina Peña,[†] Galder Kortaberria,[†] Cedric Calberg,[§] Bruno Grignard,[§] Robert Jerome,[§] Pedro M. Carrasco,[‡] David Mecerreyes,[‡] and Iñaki Mondragon*[,†]

"Materials + Technologies" Group, Polytechnic School, Dpto. Ingeniería Química y M. Ambiente, Universidad País Vasco/Euskal Herriko Unibertsitatea, Pza. Europa 1, 20018 Donostia-San Sebastián, Spain; Centre for Electrochemical Technologies (CIDETEC), Parque Tecnológico de Miramón, P° Miramón 196, 20009 Donostia-San Sebastián, Spain; and Centre for Education and Research on Macromolecules (CERM), University of Liege, Sart-Tilman, B6, 4000 Liege, Belgium

Received March 10, 2007

ABSTRACT: Novel nanostructured thermosetting materials have been prepared by modification of an epoxy resin with a semifluorinated diblock copolymer, poly(heptadecafluorodecyl acrylate)-*b*-poly(caprolactone), PaF-*b*-PCL. In a first step, the phase behavior and linear viscoelasticity of PaF-*b*-PCL were investigated. According to the segregation regime, no order−order transitions were detected, being the order−disorder transition temperature beyond the degradation temperature. Atomic force microscopy (AFM) images of the block copolymer after different thermal treatments revealed that self-assembly takes place into spherical nanodomains, which is consistent with the copolymer composition. This block copolymer was further used to prepare a nanostructured thermoset blend with an epoxy resin. DSC and DMA analysis reveals microphase separation of PaF block from the epoxy-rich phase after curing. The PaF block self-assembled into wormlike and spherical micelles in the thermoset system. This nanostructured blend presented unique surface properties showing high hydrophobicity ($\upsilon = 109°$) and low surface energy (17 mN/m).

1. Introduction

Block copolymers, BC, have been originating a great interest because of their ability to self-assemble into a variety of ordered nanoscale morphologies. The segregation of the block components is due to the thermodynamic incompatibility and the connectivity of two polymeric chains producing nanometer ordered structures.[1−9] Block copolymers are also capable of inducing self-assembling in their blends with several homopolymers leading to a variety of nanoscale morphologies.[10−13]

Block copolymers have recently been very used as templates for generating nanostructured thermosetting matrices. Several researches have reported the modification of epoxy monomers with block copolymers with long-range order in both uncured and cured states.[14−32] The aim of these modifications is mainly focused to toughen the very brittle epoxide network. One feasible pathway for generating self-assembled thermosetting nanostructures is the use of amphiphilic block copolymers, with one of the blocks miscible with the epoxy resin. In this way, poly(ϵ-caprolactone) (PCL) is a good candidate as epoxyphilic block due to its well-known miscibility with several amine-cured epoxy systems.[21,28−31] As reported by Guo et al.,[30,31] one of them is the thermosetting formulation used in the present work, diglycidyl ether of bisphenol A (DGEBA) and 4,4′-methylenebis(3-chloro-2,6-diethylaniline) (MCDEA). Recently, Meng et al.[32] reported a nanostructured system achieved by modification of a thermosetting formulation composed by DGEBA and 4,4′-methylenebis(2-chloroaniline) with an amphiphilic triblock copolymer, poly(ϵ-caprolactone)-*b*-polybutadiene-*b*-poly(ϵ-caprolactone), PCL-*b*-PB-*b*-PCL. The nanostructuring in the blend is due to the polymerization-induced microphase separation of PB domains whereas the PCL block remained mixed with the thermoset matrix.

On the other hand, fluorinated polymers have attracted recent interest due to their chemical resistance and low surface energy properties. Furthermore, these polymers present low solubility parameters leading to a marked thermodynamic incompatibility with several organic polymers. The design of block copolymers with fluorinated components in one block allows to obtain materials not only hydrophobic but lipophobic as well.[33−35] The aim of this work is to report the use of a semicrystalline poly(heptadecafluorodecyl acrylate)-*b*-poly(caprolactone) diblock copolymer, PaF-*b*-PCL, as templating agent in the development of nanostructured thermosetting materials and its unique effect in the surface properties of the nanocomposite.

2. Experimental Part

2.1. Synthesis of PaF-*b*-PCL. PaF-*b*-PCL diblock polymer was prepared under a controlled manner by the sequential ring-opening polymerization (ROP) of ϵ-caprolactone (CL) and atom transfer radical polymerization (ATRP) of heptadecafluorodecyl acrylate (aF8) in a three-step process.[36] The PCL block is first prepared by using aluminum triisopropoxide as the initiator of ROP of CL, followed by the conversion of the ω-hydroxyl end group of PCL into an activated bromine, after reaction with 2-bromopropionyl bromide. ATRP of the fluorinated methacrylate monomer is initiated from the PCL macroinitiator with a nickel-based catalyst (dibromobis(triphenylphosphine)nickel(II)) and ethyl 2-bromopropionate as initiator. Molecular mass and polydispersity index were determined by size exclusion chromatography (SEC) based on polystyrene standards, using THF as solvent. The universal calibration curve was set up on the basis of the viscosimetric relationships for PS and PCL ($[\eta]_{PS} = 1.25 \times 10^{-4}\ M^{0.717}$, $[\eta]_{PCL} = 1.09 \times 10^{-3}\ M^{0.6}$). The polydispersity index obtained for the synthesized

* Corresponding author: e-mail inaki.mondragon@ehu.es; Tel +34-943017271; Fax +34-943017200.
[†] Universidad País Vasco/Euskal Herriko Unibertsitatea.
[‡] Parque Tecnológico de Miramón.
[§] University of Liege.

10.1021/ma070585i CCC: $37.00
Published on Web 04/13/2007

Table 1. Characteristics of PaF-*b*-PCL Diblock Copolymer

block copolymer	f_{PCL}[a,b]	$M_{n,PCL}$[b] (g/mol)	$M_{n,PAF-b-PCL}$[c] (g/mol)	$T_{g,PaF}$[d] (°C)	$T_{c,PCL}$[e] (°C)	$T_{c,PaF}$[e] (°C)	$T_{m,PaF}$[e] (°C)	$T_{m,PCL}$[e] (°C)	$T_{g,PCL}$[f] (°C)	X_cPCL[g] (%)	X_c,PCLblock[g] (%)
PaF-*b*-PCL	0.89	10500	19000	−25	40	65	70	58	−55	50.3	11.7

[a] Volumetric fraction of PCL block estimated according to Helfand,[53] $f_{PCL} = (N_{PCL}/\rho_{PCL})/(N_{PCL}/\rho_{PCL} + N_{PaF}/\rho_{PaF})$, from published densities of fully amorphous PCL ($\rho_{PCL} = 1.09$ g/cm^3) and PaF monomer ($\rho_{PaF} = 1.64$ g/cm^3), being $N_{PCL} = 92$ and $N_{PaF} = 16$. [b] From ^{1}H NMR measurements (see Experimental Part). [c] From SEC analysis. [d] Glass transition temperature for PaF block measured by DSC (10 °C/min). [e] Crystallization, T_c, and melting, T_m, temperatures measured by DSC from second and third scans (1 °C/min). [f] Glass transition temperature for PCL block measured by DMA (5 °C/min). [g] Percentage of crytallinity of PCL homopolymer and PCL block in the copolymer, determined as described in the Experimental Part.

Scheme 1. ^{1}H NMR of PaF-*b*-PCL Diblock Copolymer

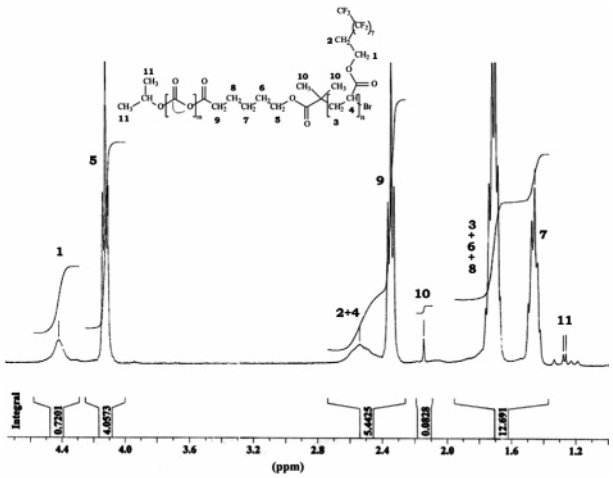

copolymer is around 1.15. The ^{1}H NMR (Bruker-500 MHz) spectrum obtained from deuterated chloroform solutions and in the CFC-113/$CDCl_3$ mixture by using tetramethylsilane, TMS, as the internal reference was used to determine the diblock copolymer weight compositions and the molecular mass of PCL block through end-group analysis. These results compare favorably with the molecular weights estimated by SEC as well as the molecular weights estimated from reaction stoichiometries.[36c] Table 1 lists the characteristics of this copolymer while the ^{1}H NMR spectrum with the corresponding assignations for the diblock copolymer is shown in Scheme 1. The PCL homopolymer was supplied by Aldrich. It has an average $M_n \sim 10\,000$ g/mol. All materials were used as received.

2.2. Thermoset Precursors. The epoxy monomer used, DER 332, was a diglycidyl ether of bisphenol A (DGEBA), supplied by Dow Chemical. It has an epoxy equivalent of around 175 and average number of hydroxyl groups per two epoxy groups $n = 0.03$. The curing agent used was an aromatic diamine, MCDEA, from Lonza. The epoxy monomer and the diamine were used in stoichiometric ratio.

2.3. Blending Protocol. 35 wt % PaF-*b*-PCL and 20 wt % PCL/epoxy systems were cured in the following way: first, the PaF-*b*-PCL or PCL and the DGEBA monomer, both containing a similar PCL weight percentage, were mixed at 150 °C until complete homogeneous mixture was obtained. MCDEA was then added to the sample with vigorous stirring for few minutes to prevent significant reaction during this step. Then the samples were degassed in vacuum and cured at 150 °C for 34 or 30 h for the PaF-*b*-PCL and PCL systems, respectively. Finally, the samples were postcured at 190 °C for 4 h.

2.4. Techniques. Differential Thermal Analysis. Thermal transition temperatures of individual components and their blends with epoxy were determined by using a differential scanning calorimeter Mettler Toledo DSC-822, under a nitrogen flow of 20 mL/min, working with 5−7 mg samples in aluminum pans. Dynamic scans were performed from −60 to 180 °C at heating/cooling rates of 1 and 10 °C/min. The percentage of crystallinity of PCL block in the copolymer has been determined from the ratio between melt enthalpy associated with melt peak of PCL in the third DSC scan (1 °C/min) and the melt enthalpy reported for PCL 100% crystalline ($\Delta H^\circ_m = 135.6$ J/g),[31] taking into account the mass percentage of PCL block in the block copolymer.

Rheological Measurements. To study the viscoelastic behavior of PaF-*b*-PCL, dynamic oscillatory shear measurements were performed using a Rheometrics Ares rheometer equipped with 13 mm diameter parallel plates and two transducers with a couple operating range of 0.02−2.000 g·cm. Parallel plates were calibrated to correct thermal expansion. Samples of 1−2 mm thickness were made by pressing the block copolymer in a press with a force of 2.5 tons. Dynamic temperature ramp tests were conducted to record the evolution of G' under isochronal conditions at a heating/cooling rate of 1 °C/min and at angular frequency of 0.1 Hz. The strain amplitude was varied from 2 to 0.05% to ensure a linear viscoelastic response.

Morphological Analysis. The morphology of the block copolymer was studied by atomic force microscopy (AFM). AFM images were obtained with a Nanoscope IIIa scanning probe microscope (Multimode, Digital Instruments). Tapping mode was employed in air using an integrated tip/cantilever (125 μm in length with ca. 300 kHz resonant frequency). Typical scan rates during recording were 0.7−1 line/s using a scan head with a maximum range of 16 × 16 μm. The specimens for AFM analysis were obtained by melting the copolymer on a slide cover at 170 °C and quenching to room temperature. Then, the obtained films were submitted to different annealing treatments, which were chosen from previous rheological measurements. Morphological features for the PaF-*b*-PCL-modified epoxy system were investigated by transmission electron microscopy (TEM), by using a Hitachi H-800-MT microscope, operated at 100 kV accelerating voltage. The samples were stained with RuO_4 vapors for 15 min to enhance contrast between the PaF and PCL/epoxy phases.

Dynamic Mechanical Analysis. The dynamic mechanical spectra (storage modulus, E', and loss factor, tan δ) of cured blends were obtained in a Perkin-Elmer DMA7 in three-point bending mode. The scans were carried out between −150 and 240 °C at a frequency of 1 Hz and a heating rate of 5 °C/min, using a span of 15 or 10 mm for the low- and high-temperature range, respectively. The samples used were parallelepipedic bars (20 × 3 × 1 mm^3). During the scans, the samples were subjected to a static force of 110 mN and a dynamic force of 100 mN.

Optical Contact Angle Measurement. Static contact angle measurements were carried out on the surface of the PaF-*b*-PCL modified and neat epoxy systems using a Data Physics OCA Series instrument. The measurements were made in air at room temperature by the sessile drop technique, water was the wetting liquid, and a drop volume of 1 μL was used. On every sample at least seven measurements were performed, placing the liquid drops in different parts of the sample surface. Droplets were maintained in contact with surface for 60 s.

3. Results and Discussion

3.1. Characterization of Diblock Copolymer. The thermal properties of PCL homopolymer and the block copolymer have been investigated by DSC (not shown here). As shown in Table 1, the crystallization and melting processes of the block copolymer occurred in two stages under the conditions employed, thus suggesting that both PCL and PaF crystallize in

the block material. The percentage of crystallinity of PCL blocks is much lower than that of pure PCL probably because PCL blocks crystallize under stress in the PaF semicrystalline network formed at higher temperature.[37,38] Although not shown, the melting/crystallization process has also been followed by optical microscopy (OM), confirming DSC measurements.

Regarding the phase behavior of the block copolymer, a crude estimation of the segment−segment interaction parameter has been done. It is well-known that for the block copolymer case the Flory−Huggins interaction parameter χ can be approximated in terms of solubility parameters of both blocks, thus obtaining the χN values from[39]

$$\chi N \approx (\delta_1 - \delta_2)^2 (V/RT) \quad (1)$$

where N is the average polymerization degree, $\delta_{1(2)}$ are solubility parameters of each block, V is the molar volume, and R is the gas constant. According to the Hoftyzer−Van Krevelen method,[40] the values of $\delta_{1(2)}$ are 14.6 (19.8) $MPa^{1/2}$ for PaF (PCL), which agree with that reported by other authors,[41] and then a value of $\chi N \sim 170$ at 298 K is obtained, which puts the copolymer in the strong segregation regime. Consequently, the morphology will basically depend on the volumetric fraction of the minority block.[39,42] Rheological measurements have confirmed the segregation regime of the PaF-*b*-PCL copolymer. Figure 1a shows the specifics changes in low-frequency dynamic moduli G' profile through the heating−cooling−heating cycle. As the possible thermal transformations, OOT and ODT, could be affected by melting/crystallization processes, the corresponding DSC scans are shown in the inset. An increase of the magnitude of G' can be observed in the first heating scan to finally reach a plateau value, which is maintained in the following cooling/heating scans before and after the corresponding melting/crystallization processes. Moreover, during the second heating scan and after the melting process of PCL block, the plateau of G' is maintained until around 240 °C, the temperature at which degradation reactions were detected by TGA (not show here), which evidences, in agreement with the strong segregation regime of the block copolymer,[42] that the ODT for this copolymer is over its degradation temperature. Taking into account that the copolymer is strongly segregated, the increase of G' will be presumably a consequence of block copolymer ordering. In fact, by comparing the first heating scan with the corresponding one to a sample previously annealed 24 h at 80 °C, G' evolution revealed that the unannealed sample required higher temperature to overtake the plateau than the stabilized sample (Figure 1b). Thus, the observed behavior in the magnitude of G' might be attributed to ordering of PaF-*b*-PCL copolymer during the heating scan.

Figure 2 shows the AFM images of PaF-*b*-PCL films submitted to different annealing treatments, which have been chosen according to rheological measurements. As can be observed, PaF-*b*-PCL copolymer presents self-assembling into PaF spherical nanodomains, with average diameter ranging from 40 to 80 nm, in a PCL matrix for all the annealing treatments employed, which is consistent with the volumetric fraction of PaF block of 15%. Even taking into account that film behavior can differ from the corresponding one to bulk morphology, this fact seems to indicate that the changes in G' value observed in rheological measurements are just a consequence of the ordering dynamics since the copolymer appears strongly segregated.

3.2. Characterization of the Nanostructured Thermosetting Systems. Interestingly, the PaF-*b*-PCL-modified epoxy systems were transparent at ambient temperature after curing, thus suggesting the absence of macroscopic phase separation

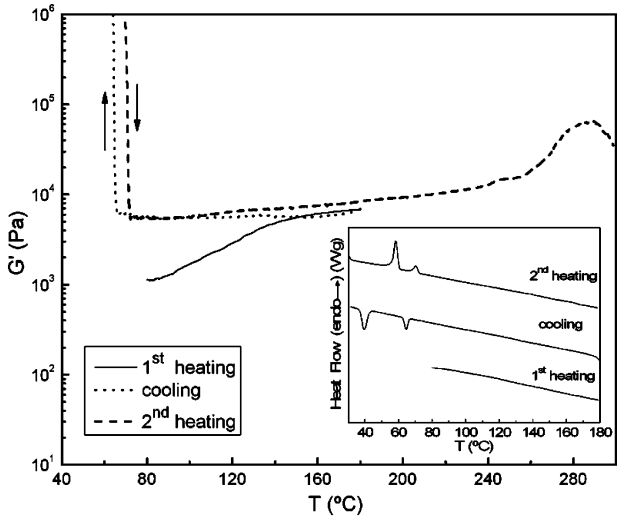

(a)

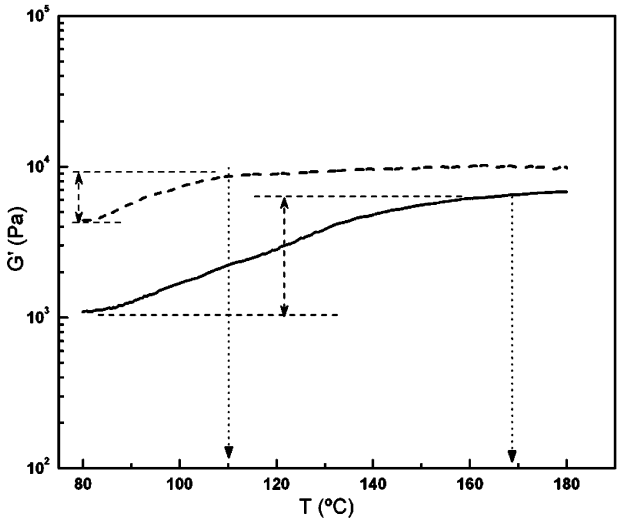

(b)

Figure 1. Isochronal temperature dependence of the storage modulus (G') of PaF-*b*-PCL diblock copolymer at a frequency of 0.1 Hz from the melted state. (a) During heating−cooling−heating process. (b) During heating process: (- -) sample annealed at 80 °C, 24 h, and (—) sample without previous annealing (first heating scan shown in (a)). Strain-amplitude used varies from $\gamma_0 = 0.05-2\%$ to ensure linear viscoelastic response. The inset in (a) shows the corresponding DSC dynamic scans in nitrogen atmosphere. Scan rate 1 °C/min.

in the blends. To ascertain the mixing degree of the cross-linked epoxy networks with PCL and PaF blocks, DSC and DMA techniques have been employed. The DSC thermograms of individual components and modified epoxy networks after curing are shown in Figure 3a,b, while the real values of the heat of melting and crystallization are shown in Table 2. The PaF-*b*-PCL exhibits two evident melting/crystallization peaks, attributable to the semicrystalline PaF and PCL blocks. For 20 wt % PCL-modified epoxy system, a small melting/crystallization peak appears, indicating some degree of crystallinity in the blend, which taking into account the enthalpy values given in Table 2 can be considered as residual. As mentioned above, PCL has been found miscible in the DGEBA/MCDEA system before and after curing reaction.[30,31] For the PaF-*b*-PCL-modified system, no melting/crystallization peak for PCL block appears. It is plausible to propose that the PCL blocks were interpenetrated in the cross-linked epoxy networks due to the well-known PCL miscibility with epoxy networks.[32,43,44] Mis-

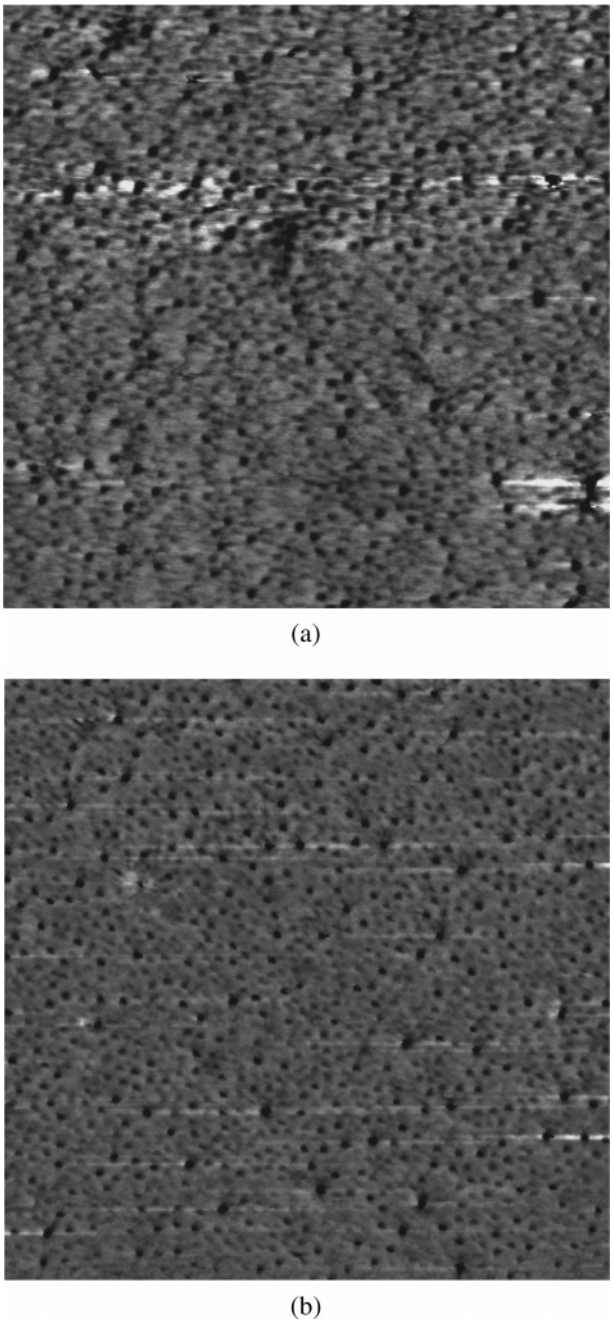

Figure 2. TM-AFM topographical images of PaF-*b*-PCL films annealed at (a) 80 °C, 20 h + 80 − 180 − 80 °C, $\upsilon = 1$ °C/min, and (b) 120 °C, 48 h. Image size 5 μm × 5 μm.

cibility has been further confirmed by the changes in glass transition temperatures. While the neat epoxy matrix displays a glass transition temperature of 177 °C, the PaF-*b*-PCL- and PCL-modified epoxy systems display a T_g which shifts down to lower temperature, thus indicating that both PCL and PaF-*b*-PCL are at least partially miscible in the epoxy matrix. The presence of hydrogen-bonding interactions between the hydroxyl groups of epoxy and the carbonyl group of PCL has been confirmed by FTIR. Furthermore, the melting peak of PaF block remained slightly unaffected in the epoxy blend, thus suggesting that the PaF block could be separated out from the epoxy matrix. The corresponding crystallization process, however, occurs at lower rate of crystallization than in the neat copolymer, which might be a consequence of two differently domains of PaF block present in this blend but also to the fact that crystallization of PaF blocks could be greatly slowed in nanoscale confined

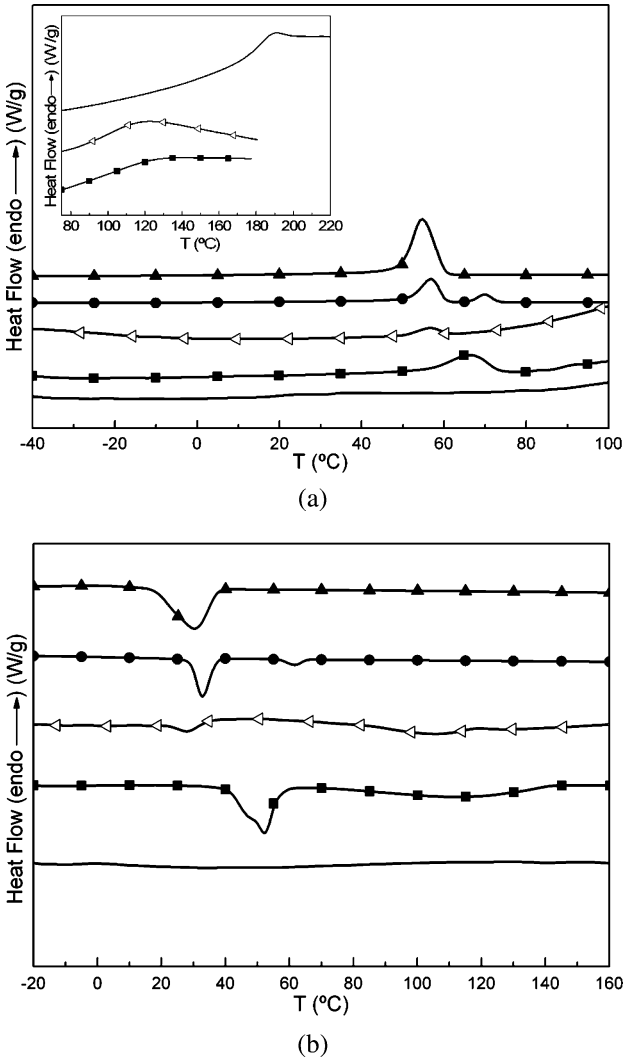

Figure 3. DSC dynamics runs at 10 °C/min in nitrogen atmosphere of (▲) PCL homopolymer and (●) PaF-*b*-PCL diblock copolymer and cured DGEBA/MCDEA systems for (—) neat epoxy, (△) 20 wt % PCL, and (■) 35 wt % PaF-*b*-PCL. (a) Heating and (b) cooling scans. The inset shows the corresponding heating scan at high range temperature. In all cured systems the heat flow was multiplied by a factor of 14. Values of the heat of melting and crystallization are shown in Table 2.

Table 2. Thermal Properties from DSC Measurements of PCL Homopolymer, PaF-*b*-PCL Diblock Copolymer, and Cured DGEBA/MCDEA Systems for 20 wt % PCL and 35 wt % PaF-*b*-PCL

designation	ΔH_m[a] (J/g)	ΔH_c[b] (J/g)
PCL homopolymer	73.4	76.4
PaF block in the copolymer	6.2	6.8
PCL block in the copolymer	25.5	25.5
20 wt % PCL/epoxy system	0.3	0.1
35 wt % PCL-block/epoxy system		
35 wt % PaF-block/epoxy system	1.4	1.7

[a] Normalized melt enthalpy (ΔH_m) from DSC measurements. Scan rate of 10 °C/min. [b] Crystallization enthalpy (ΔH_c) from DSC measurements. Scan rate of 10 °C/min.

environments.[17] Thus, the significantly higher temperature range of the glass transition in the block copolymer-modified system could be attributed to the enrichment of PCL chains around PaF domains.[32]

Dynamic mechanical analysis carried out in fully reacted samples is shown in Figure 4a,b, where the corresponding spectra for neat PCL homopolymer and PaF-*b*-PCL copolymer in the low-temperature range have been included for comparison. The neat epoxy system exhibits two relaxation processes: (i) a

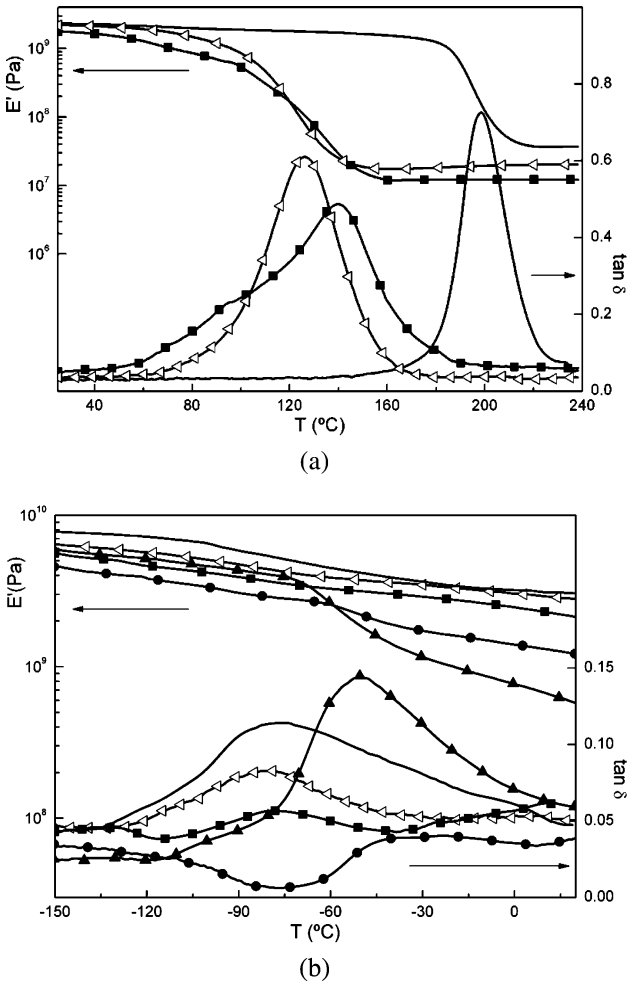

Figure 4. Dynamic mechanical spectra obtained at 1 Hz of neat DGEBA/MCDEA system (—) and its blends containing (△) 20 wt % PCL and (■) 35 wt % PaF-*b*-PCL. (a) High- and (b) low-temperature range. For comparison, spectra for neat PCL homopolymer (▲) and PaF-*b*-PCL diblock copolymer (●) have been included in the low-temperature range.

low-temperature relaxation (around −80 °C), corresponding to β relaxation mode, associated with localized motions of the glycerol groups and the diphenylpropane units,[45,46] and (ii) a relaxation at 190 °C, which corresponds to the α relaxation mode, associated with glass transition temperature. Spectra for blends containing 20 wt % PCL and 35 wt % PaF-*b*-PCL showed a shift of α relaxation of the epoxy-rich phase to lower temperatures. The values of the glass temperatures agree with the corresponding ones obtained by the equation of Gordon−Taylor,[47] which indicates that the shift of the α relaxation is related to the full dissolution of 20 wt % PCL.[30] In addition, the slightly higher values for block copolymer-modified system could be related to both a restriction in the mobility of PCL chains in the copolymer and a partial deswelling of PCL chains due to the microphase separation of PaF block. Taking into account the results obtained by other authors,[18,19] it can be assumed that part of PCL, near the PaF immiscible block, can deswell and is not yet soluble in the epoxy matrix. Indeed, the broadening of the α relaxation could be attributed to the appearance of a shoulder around 80 °C because of the melting of the PaF block. Furthermore, although the T_g of PCL falls in the same temperature range that the β relaxation of epoxy-rich phase, it seems not to appear in the spectrum of both modified epoxy systems. Nevertheless, the T_g for PaF block in the 35 wt % PaF-*b*-PCL-modified epoxy system, which appears around

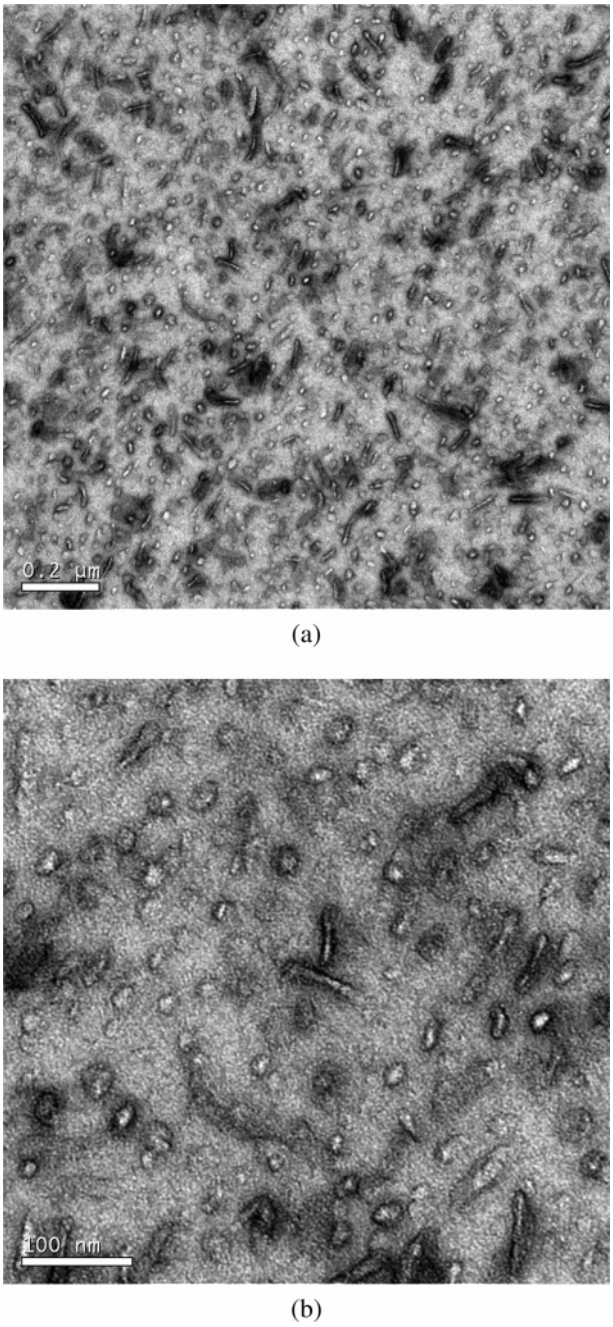

Figure 5. TEM images at different magnifications on different regions for DGEBA/MCDEA cured blend containing 35 wt % PaF-*b*-PCL. The samples have been stained with RuO_4 for 4 min. Scale bar: (a) 0.2 μm and (b) 100 nm.

−25 °C overlapped with the corresponding one to PCL block in neat block copolymer, appears to be practically unaffected by the epoxy network, thus confirming phase separation between PaF block and the epoxy-rich phase (Figure 4b).

TEM micrographs for this system (Figure 5) clearly show nanostructuring through microphase separation, where wormlike and spherical micelles with an average size in length of about 70 and 20 nm, respectively, are dispersed in a continuous epoxy resin matrix. Because of the RuO_4 staining, amorphous PCL appears darker in the TEM images,[48] while white and gray domains correspond to PaF and the epoxy-rich phase, respectively. This structure remained stable after 3 months as the nanodomains were fixed inside the epoxy matrix.

Last and interestingly, the surface properties of this novel nanostructured blend have been investigated by contact-angle

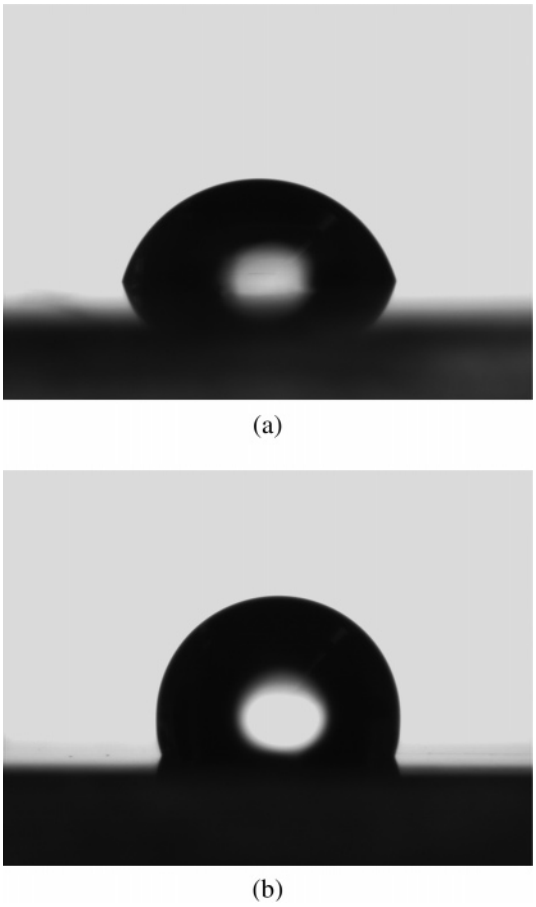

Figure 6. Images of a water droplet in contact with (a) neat DGEBA/MCDEA system and (b) its blend containing 35 wt % PaF-*b*-PCL. Droplets in contact with surface for 60 s.

measurements (Figure 6). Surface free energies of both 35 wt % PaF-*b*-PCL-modified epoxy and neat epoxy systems have been calculated from contact angle data using the equation-of-state theory.[49,50] Results so obtained show that the modified system has a higher hydrophobicity ($\upsilon = 109°$) and low surface energy (17 mN/m) in comparison with the neat epoxy system, which exhibits low water repellence ($\upsilon = 73°$) and high surface energy (39 mN/m). This fact indicated that the fluorinated polymer is present at the surface of the epoxy mixture. Previous studies with other fluorinated mixtures[51,52] have shown that the air−blend interface is mainly occupied by the fluorinated chains because these chains can easily migrate to the uppermost surfaces of the blends, even with only 1.5 wt % of the fluorinated component in the blends.

4. Conclusions

In the present study, we have reported the thermal and phase behavior of a synthesized semicrystalline PaF-*b*-PCL diblock copolymer. The PaF-*b*-PCL has been successfully used to prepare nanostructured thermoset blends, resulting in microphase separation of PaF chains from the epoxy-rich phase containing mostly PCL block, as demonstrated by DSC and DMA measurements. TEM images revealed that self-assembling process leading to nanostructured thermoset blend takes place into spherical and wormlike PaF micelles, which is consistent with the copolymer composition and content in the blend. That novel nanostructured epoxy blend is a material with low surface energy and high water repellence.

Acknowledgment. The authors thank funding from Basque Government, NANOTRON project, "Ministerio de Ciencia y Tecnología" for its support through projects MAT2003-08125. We also acknowledge the support of EU NoE Nanofun-Poly.

References and Notes

(1) Bates, F. S.; Fredrickson, G. H. *Annu. Rev. Chem.* **1990**, *41*, 525−557.
(2) Han, C. D.; Baek, D. M.; Kim, J. K.; Ogawa, T.; Hashimoto, T. *Macromolecules* **1995**, *28*, 5043−5062.
(3) Matsen, M. W.; Bates, F. S. *Macromolecules* **1996**, *29*, 1091−1098.
(4) Hillmyer, M. A; Bates, F. S. *Macromol. Symp.* **1997**, *117*, 121−130.
(5) Alexandridis, P.; Lindman, B. *Amphiphilic Block Copolymers: Self Assembly and Applications*; Elsevier: New York, 2000.
(6) Hadjichristidis, N.; Pispas, S.; Floudas, G. A. *Block Copolymer*; John Wiley & Sons: New York, 2003.
(7) Lodge, T. P. *Macromol. Chem. Phys.* **2003**, *204*, 265−273.
(8) Hamley, I. W. *Developments in Block Copolymer Science and Technology*; John Wiley & Sons, Ltd.: London, UK, 2004.
(9) Ryu, D. Y.; Lee, D. H.; Jeong, U.; Yun, S. H.; Park, S.; Kwon, K.; Sohn, B. H.; Kim, J. K. *Macromolecules* **2004**, *37*, 3717−3724.
(10) Paul, D. R., Newman, S., Eds.; In *Polymer Blends*; Academic Press: New York, 1978; Vol. 1.
(11) Matsen, M. W. *Macromolecules* **1995**, *28*, 5765−5773.
(12) Koning, C.; Duin, M. V.; Pagnoulle, C.; Jérôme, R. *Prog. Polym. Sci.* **1998**, *23*, 707−757.
(13) Park, M. J.; Bang, J.; Harada, T.; Char, K.; Lodge, T. P. *Macromolecules* **2004**, *3*, 9064−9075.
(14) Lipic, P. M.; Bates, F. S.; Hillmyer, M. A. *J. Am. Chem. Soc.* **1998**, *120*, 8963−8970.
(15) Grubbs, R. B.; Dean, J. M.; Broz, M. E.; Bates, F. S. *Macromolecules* **2000**, *33*, 9522−9534.
(16) Guo, Q.; Thomann, R.; Gronski, W.; Thurn-Albrecht, T. *Macromolecules* **2002**, *35*, 3133−3144.
(17) Guo, Q.; Thomann, R.; Gronski, W.; Staneva, R.; Ivanova, R.; Stühn, B. *Macromolecules* **2003**, *36*, 3635−3645.
(18) Ritzenthaler, S.; Court, F.; David, L.; Girard-Reydet, E.; Leiber, L.; Pascault, J. P. *Macromolecules* **2002**, *35*, 6245−6254.
(19) Ritzenthaler, S.; Court, F.; David, L.; Girard-Reydet, E.; Leiber, L.; Pascault, J. P. *Macromolecules* **2003**, *36*, 118−126.
(20) Dean, J. M.; Verghese, N. E.; Pham, H. Q.; Bates, F. S. *Macromolecules* **2003**, *36*, 9267−9270.
(21) Dean, J. M.; Grubbs, R. B.; Saad, W.; Cook, R. F.; Bates, F. S. *J. Polym. Sci., Part B: Polym. Phys.* **2003**, *41*, 2444−2456.
(22) Girard-Reydet, E.; Pascault, J. P.; Bonnet, A.; Court, F.; Leibler, L. *Macromol. Symp.* **2003**, *198*, 309−322.
(23) Rebizant, V.; Abetz, V.; Tournilhac, F.; Court, F.; Leibler, L. *Macromolecules* **2003**, *36*, 9889−9896.
(24) Rebizant, V.; Venet, A. S.; Tournilhac, F.; Girard-Reydet, E.; Navarro, C.; Pascault, J. P.; Leibler, L. *Macromolecules* **2004**, *37*, 8017−8027.
(25) Serrano, E.; Tercjak, A.; Kortaberria, G.; Pomposo, J. A.; Mecerreyes, D.; Zafeiropoulos, E.; Stamm, M.; Mondragon, I. *Macromolecules* **2006**, *39*, 2254−2261.
(26) Wu, J.; Thio, Y. S.; Bates, F. S. *J. Polym. Sci., Part B: Polym. Phys.* **2005**, *43*, 1950−1965.
(27) Thio, Y. S.; Wu, J.; Bates, F. S. *Macromolecules* **2006**, *39*, 7187−7189.
(28) Chen, J. L.; Huang, H. M.; Li, M. S.; Chang, F. C. *J. Appl. Polym. Sci.* **1999**, *71*, 75−82.
(29) Chen, J. L.; Chang, F. C. *Macromolecules* **1999**, *32*, 5348−5356.
(30) Guo, Q.; Harrats, C.; Groeninkx, G.; Reynaers, H.; Koch, M. H. *Polymer* **2001**, *42*, 6031−6041.
(31) Guo, Q.; Groeninkx, G. *Polymer* **2001**, *42*, 8647−8655.
(32) Meng, F.; Zheng, S.; Zhang, W.; Li, H.; Liang, Q. *Macromolecules* **2006**, *39*, 711−719.
(33) Iyengar, D. R.; Perutz, S. M.; Dai, C.-A.; Ober, C. K.; Kramer, E. J. *Macromolecules* **1996**, *29*, 1229−1234.
(34) Toselli, M.; Messori, M.; Bongiovanni, R.; Malicelli, G.; Priola, A.; Pilati, F.; Tonelli, C. *Polymer* **2001**, *42*, 1771−1779.
(35) Xu, J.; Ni, P.; Mao, J. *e-Polym.* **2006**, *no. 015*.
(36) (a) Hawker, C. J.; Hedrick, J. L.; Malmstrom, E. E.; Trollsas, M.; Mecerreyes, D.; Moineau, G.; Dubois, P.; Jerome, R. *Macromolecules **1998**, 31*, *213*−219. (b) Stassin, F. Ph.D. Thesis, University of Liège, Belgium, 2005. (c) Fabrice, S.; Bruno, G.; Cédric, C.; Jérôme, R. *Macromolecules*, submitted.
(37) Lefèvre, C.; Villers, D.; Koch, M. H. J.; David, C. *Polymer* **2001**, *24*, 8769−8777.
(38) Nojima, S.; Akutsu, Y.; Akaba, M.; Tanimoto, S. *Polymer* **2005**, *46*, 4060−4067.
(39) (a) Bates, F. S.; Fredickson, G. H. *The Physics of Block Copolymers*; Hamley, I., Ed.; Oxford University Press: Oxford, UK, 1998. (b) Hashimoto, T. In *Thermoplastic Elastomers. A Comprehensive Review*; Legge, N. R., Holden, G., Schroeder, H. E., Eds.; Munich: Hanser, 1987.

(40) Van Krevelen, D. W. *Properties of Polymers*; Elsevier Scientific Publishing Co.: Amsterdam, 1990.
(41) Granville, A. M.; Boyes, S. G.; Akgun, B.; Foster, M. D.; Brittain, W. J. *Macromolecules* **2004**, *37*, 2790−2796.
(42) (a) Helfand, E.; Wasermann, Z. R. In *Developments in Block Copolymers*; Goodman, I., Ed.; Applied Science: New York, 1982; Vol. 1. (b) Weidisch, R.; Schreyeck, G.; Ensslen, M.; Michler, G. H.; Stamm, M.; Schubert, D. W.; Budde, H.; Arnold, M.; Jerome, R. *Macromolecules* **2000**, *33*, 5495−5504.
(43) Zheng, S.; Zheng, H.; Guo, Q. *J. Polym. Sci., Part B: Polym. Phys.* **2003**, *41*, 1085−1098.
(44) Zheng, S.; Lü, H.; Chen, C.; Nie, K.; Guo, Q. *Colloid Polym. Sci.* **2003**, *281*, 1015−1024.
(45) Federolf, H. A.; Eyerer, P.; Moginger, P.; Mebus, C.; Jin, R.; Scheer, W. *J. Polym. Sci., Part B: Polym. Phys.* **1999**, *19*, 243−263.
(46) Gerard, J. F. *Polym. Eng. Sci.* **1998**, *28*, 568−577.
(47) Gordon, M.; Taylor, J. S. *J. Appl. Chem.* **1952**, *2*, 495.
(48) Zhao, Y. F.; Fan, X.; Chen, X.; Wan, X.; Zhou, Q. F. *Polymer* **2005**, *46*, 5396−5405.
(49) Neumann, A. W.; Spett, J. K.; Neumann, N. *Applied Surface Thermodynamics*; M. Dekker: New York, 1996.
(50) Long, J.; Chen, P. *Langmuir* **2001**, *17*, 2965−2972.
(51) Tan, H.; Guo, M.; Du, R.; Xie, X.; Li, J.; Zhong, Y.; Fu, Q. *Chin. J. Polym. Sci.* **2004**, *2*, 559−566.
(52) Huang, H. L.; Goh, S. H.; Lai, D. M. Y.; Wee, A. T. S.; Huan, C. H. A. *J. Polym. Sci., Part B: Polym. Phys.* **2004**, *42*, 1145−1154.
(53) Helfand, E. *Macromolecules* **1975**, *8*, 552−556.

MA070585I